Armenian Journal of Physics, 2021, vol. 14, issue 1, pp. 8-18

Cobalt Doped SnO_2 Thin Film for Detection of Vapor Phase Hydrogen Peroxide

https://doi.org/10.52853/18291171-2021.14.1-8

M.S. Aleksanyan[1], V.M. Aroutiounian[1], G.E. Shahnazaryan[1], A.G. Sayunts[1]

[1]*Yerevan State University, 1 Alex Manoukian str., 0025, Yerevan, Republic of Armenia*

E-mail: maleksanyan@ysu.am

Received 3 March 2021

Abstract. A technology was developed for manufacturing solid-state semiconductor sensor sensitive to hydrogen peroxide vapors. Gas sensitive nanostructured films made of doped metal oxide SnO_2<Co> were manufactured by the high-frequency magnetron sputtering method. The chemical composition of prepared SnO_2<Co> targets was analyzed and the thickness of the deposited doped metal oxide film was measured. The morphology of the deposited Co-doped SnO_2 film was studied by scanning electron microscopy. The gas sensing characteristics to the different concentrations of hydrogen peroxide vapors at various operating temperatures were also studied. The Co-doped SnO_2 sensor showed enough sensitivity to very low concentration of hydrogen peroxide vapors (875 ppb) at the operating temperature of 100 °C. The SnO_2<Co> based sensor can be successfully used in medical diagnostic apparatus for determining low concentration of hydrogen peroxide vapors in exhaled air.

Keywords: Sensor, nanostructured film, semiconductor, metal oxide, hydrogen peroxide vapors.

1. Introduction

Hydrogen peroxide (H_2O_2) is a colorless liquid dissolved with water in all proportions. It is unstable and can easily break down into water and oxygen producing energy. It is known as a good oxidizing agent and can cause spontaneous combustion when comes in contact with organic material. In some cases, H_2O_2 or its vapors can be dangerous for human health. Brief contact of H_2O_2 with the skin leads to irritation and whitening. The extent of the hazard is determined by the concentration of the H_2O_2 solution. Contact with the eyes can lead to serious injury and drinking a weak solution of H_2O_2 may cause severe gastrointestinal effects [1].

H_2O_2 has a wide application fields in different area. It can be used as an anti-bacterial agent in the medical field. It can be also used for disinfection and sterilization in everyday life and industry. It is utilized in chemical industry, manufacturing of organic products, mining industry for extraction uranium from ores, analytical chemistry, rocketry, bipropellant systems and so on.

As mentioned, H_2O_2 serves as a disinfectant for medical equipment and surfaces as well as for sterilizing of surgical instruments. The process of decontamination can be carried out in different ways: mechanical, chemical, physical, and physicochemical ways. The chemical decontamination which has many advantages, in turn, is divided into two groups: wet decontamination (water solution of

$ClO_2, H_2O_2, NaOCl$ and so on) and dry decontamination (vapor or gas phase of H_2O_2, ClO_2, O_3 and so on). The "ideal decontamination agent" should be non-toxic to humans and environment, compatible with different materials, easily detectable and cheaper. The best candidate for "ideal decontamination agent" is the H_2O_2 in vapor phase. It is able to sterilize a wide range of microorganisms. It has also high germicidal activity. The correct selection of the H_2O_2 concentration during the sterilization of the equipment and technological surfaces as well as the control of the H_2O_2 content in air after completion of disinfection cycle are very important. Therefore, the development and manufacturing of stable and reproducible sensors sensitive to H_2O_2 vapors are extremely required [2-9].

There are many methods to detect and analyze of H_2O_2 vapors including gas chromatography, Fourier-transform infrared spectroscopy, chemiluminescence detectors, mass spectrometry, semiconductor gas sensors and so on. Solid-state gas sensors made of metal oxide semiconductors (MOSs) have many advantages in comparison to other gas sensing methods. These are used to monitor the content of oxidizing and reducing gas molecules in the environment. MOSs gas sensors have been widely studied due to their low costs, easy to miniaturize and production, high stability and reliability. The metal oxide based resistive sensors can be designed to operate under different conditions including high temperatures, chemically active environment, in humid conditions and so on [10-15].

As a typical $n-$type MOS, tin oxide (SnO_2) with a wide band-gap energy (3.6 eV) has been widely used in solid-state gas sensors due to its low cost, non-toxicity, easy-achieved real-time response in gas-sensing application, low operating temperatures, high sensitivity, high reactivity to reducing gases at relatively low operating temperatures and easy adsorption of oxygen at the surface because of the natural non-stoichiometry. In the last decades, SnO_2 is considered the most widely used and studied material in the field of gas sensors. The conductivity of SnO_2 based sensor increases in the presence of a reducing gases, and decreases in the presence of an oxidizing gas [16, 17].

As mentioned above, pure SnO_2 is an n-type semiconductor due to the presence of the native donor levels. However, pure SnO_2 exhibits low sensitivity, poor selectivity and high electrical resistance. In order to improve the chemical, physical and gas sensing properties of the SnO_2, noble metals and different additives are imported [18-20].

In this study, we prepared Co doped ZnO based sensor for detection of hydrogen peroxide vapor and confirmed its high sensitivity by means of gas sensing studies.

2. Sensors preparation and material characterization

Ceramic targets made of metal oxide SnO_2 doped with 2 at.% Co were synthesized by the solid-phase reaction method [21]. The compacted $SnO_2 < Co >$ samples were exposed to thermal treatment in the programmable furnace Nabertherm, HT O4/16 with the controller of C 42. The annealing was carried out at 500 °C, 700 °C, 1000 °C and 1100 °C consecutively, soaking at each temperature for 5 h (Table 1). Then the compositions were subjected to mechanical treatment in the air in order to eliminate surface defects. Thus, smooth parallel targets with a diameter of $40mm$ and thickness of $2mm$ were prepared (Fig. 1).

Table 1. The annealing steps of SnO_2 doped with 2 at.% Co ceramic target.

No.	Annealing temperature, ^0C	Annealing time, hour
1.	25 - 500	4
2.	500	5
3.	500 - 700	1
4.	700	5
5.	700 - 1000	1
6.	1000	5
7.	1000 - 1100	1
8.	1100	5
9.	1100 - 25	10

The chemical composition of prepared $SnO_2 < Co >$ targets was studied using the Niton™ XL3t GOLDD+ XRF Analyzer. The results of this investigation have shown that the real content of cobalt's atoms in the prepared ceramic targets was equal to $1.3at.\%$. So, ceramic targets with compositions of $Sn_{0.987}Co_{0.013}O_2$, were synthesized.

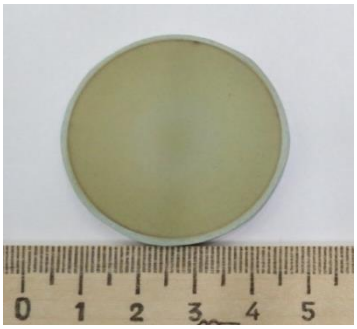

Fig. 1. The photo of the ceramic target based on SnO_2 doped with 2 at.% Co (with cm unit).

Prepared semiconductor $SnO_2 < Co >$ targets were used for deposition of nanosized films on the Multi-Sensor-Platforms by the high-frequency magnetron sputtering method. The platform integrates a temperature sensor $(Pt\,1000)$, a heater and interdigitated platinum electrodes on a ceramic substrate. The heater and temperature sensor were covered with an insulating glass layer. Gas sensitive layer made of $Sn_{0.987}Co_{0.013}O_2$ was deposited onto the non-passivated electrode structures. That way the Multi-Sensor-Platform was converted into gas sensor (Fig. 2).

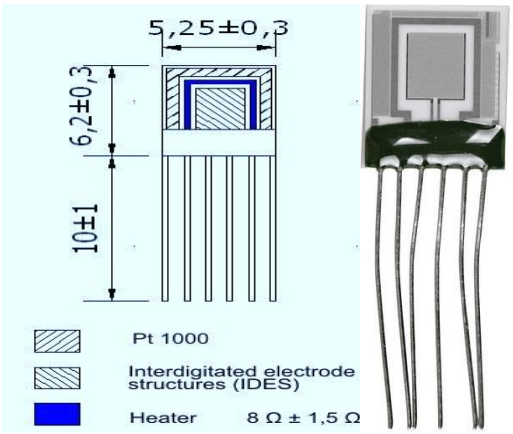

Fig. 2. The schematic diagram (with mm unit) and photo of the Multi-Sensor-Platform.

The following working conditions of the high-frequency magnetron sputtering were chosen: the power of the magnetron generator unit was $60W$; the substrate temperature during the sputtering was 200^0C and the duration of the sputtering process was equal to 20 minutes. The sensing device was completed through the ion-beam sputtering deposition of palladium catalytic particles (the deposition time was 3 seconds). Further annealing of the manufactured structures was carried out at the temperature of 250^0C during 2 hours in the air to obtain homogeneous films and eliminate mechanical stresses.

The thickness of the deposited film was measured by the Alpha-Step D-100 (KLA Tencor) profiler. The result of study of the film -substrate transition profile is shown in Fig. 3. The thickness of the $SnO_2 < Co >$ film was equal to 138 nm.

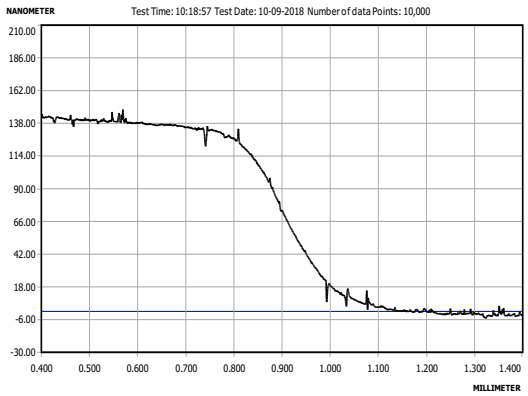

Fig. 3. The $Sn_{0,987}Co_{0,013}O_2$ film thickness measurement result.

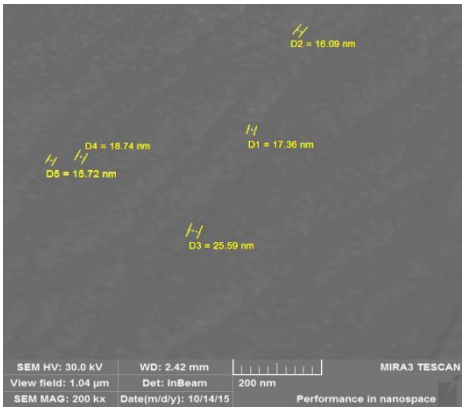

Fig. 4. The SEM image of the $Sn_{0,987}Co_{0,013}O_2$ film.

The sensing properties of the resistive sensors depend on the microstructure of the sensing material, especially on the porosity and grain size [22-25]. The morphology of the deposited Co-doped SnO_2 films was studied by scanning electron microscopy using Mira 3 LMH (Tescan). The average size of nanoparticles was approximately $18.7nm$ (Fig. 4).

3. Experimental Results and Discussion

The sensing mechanism of n-type ($SnO_2 < Co >$ is an n-type semiconductor metal oxide) semiconductor gas sensors can be explained by modulation model of surface electron depletion layer or modulation of inter-grain barrier. Commonly, when the doped $SnO_2 < Co >$ layer is exposed to air, ambient oxygen molecules or atoms adsorb on the sensor surface and capture the conduction-band electrons to become chemisorbed active ionic species of oxygen. Thus, an electron depletion layer is formed near the $SnO_2 < Co >$ sensor surface and we have an increasing in the resistance of semiconductor resistive thin film. When the target oxidizing gas molecules (H_2O_2) are introduced to surface of the sensor, there are dissociated on the surface of semiconductor and supplemented by additional oxygen atoms. These additional atoms capture the conduction-band electrons increasing the resistance of the $SnO_2 < Co >$ thin film.

The gas sensing properties of the prepared sensors under the influence of H_2O_2 vapors were investigated using an internally developed and computer-controlled static gas sensor test system [26]. The sensitivity of the $SnO_2 < Co >$ sensor to the different concentrations of H_2O_2 vapors was measured at various operating temperatures. The sensor response was determined as the ratio of R_{gas}/R_{air}, where R_{gas} is the resistance in the presence of target gas in the air and R_{air} is the resistance in the air without target gas.

The $SnO_2 < Co >$ sensor exhibited a sufficient sensitivity to H_2O_2 vapors even at room temperature. The resistance of the sensor increases by 2.2 and 8 times at the presence of H_2O_2 vapors with the concentration of $3.5ppm$ and $105ppm$, respectively (response times were 10 and 5 minutes, respectively) at operating temperature of 25^0C. The typical results of measurements of changes in the resistance of the $SnO_2 < Co >$ sensor at low operating

temperatures are presented in Fig. 5. As shown, the resistance of the sensor does not return to its initial value after the gas is eliminated, and the additional heating is required to overcome this problem.

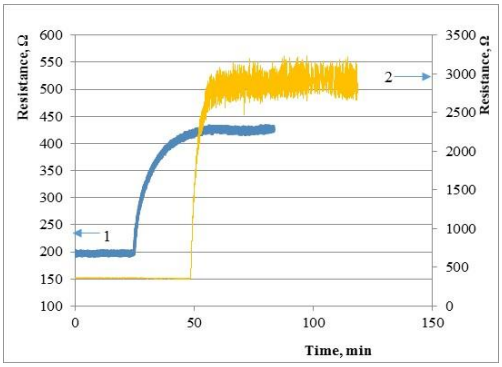

Fig. 5. The response-recovery curves of SnO_2<Co> sensor observed under the influence of 3.5 ppm (1) and 105 ppm (2) of H_2O_2 vapors at 25 ºC operating temperature.

The temperature vs. resistance curve for nanostructured $SnO_2 < Co >$ film (in the air) was extracted. It is known that the resistance of semiconductor decreases with the increase of temperature, which is due to the increasing of the concentration of free carriers in the conduction band. In case of thin films, the situation is somewhat different. The temperature of thin film increases with the decreasing of the resistance and starting at a certain temperature rises again reaching its saturation value. The dependence of the resistance of the $SnO_2 < Co >$ film on temperature in the air is presented in Fig. 6.

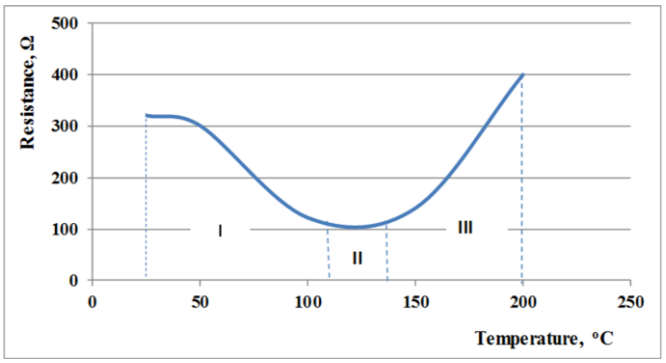

Fig. 6. The temperature vs. resistance curve for SnO_2<Co> film.

As can see, the temperature dependence of the film's resistance shows so-called three-region behavior. The resistance drop in the first region is due to the generating of electrons in the conduction band as a result of thermal excitation, as in ordinary bulk semiconductors. The temperature effect in the second region is rather small and there is a competition between electrons generation process and the surface adsorption of active oxygen. So, there is a balance between the thermal excitation and oxygen adsorption processes. The increasing of the resistance in the third region is due to the increasing of adsorption rate of active oxygen on the surface of the thin film. So, the operating temperature of the sensor should be selected in the region where

the oxygen adsorption and desorption processes are performed faster and more intensely.

The responses of the $SnO_2 < Co >$ sensor to the H_2O_2 vapors at different operating temperatures were also measured. Even at extremely low concentrations ($875\,ppb$), the responses of the sensor were 2.8 and 2.15 at 100 and 150^0C operating temperatures, respectively (Fig. 7a). The response times were equal to 4.5 and 1.08 minutes at 100 and 150^0C operating temperature, respectively, and the recovery times were equal to 41.8 and 6 minutes at 100 and 150^0C operating temperature, respectively. So, the response value of the $SnO_2 < Co >$ sensor was higher at $75, 100$ and 125^0C operating temperatures than that of at 150^0C operating temperature, but from the point of view of high performance the 150^0C was chosen as an optimal operating temperature. This conclusion is confirmed by the results of measurements of the $SnO_2 < Co >$ sensor sensitivity to H_2O_2 vapors with $3.5\,ppm$ concentration at different operating temperatures (Fig. 7b and Fig. 8).

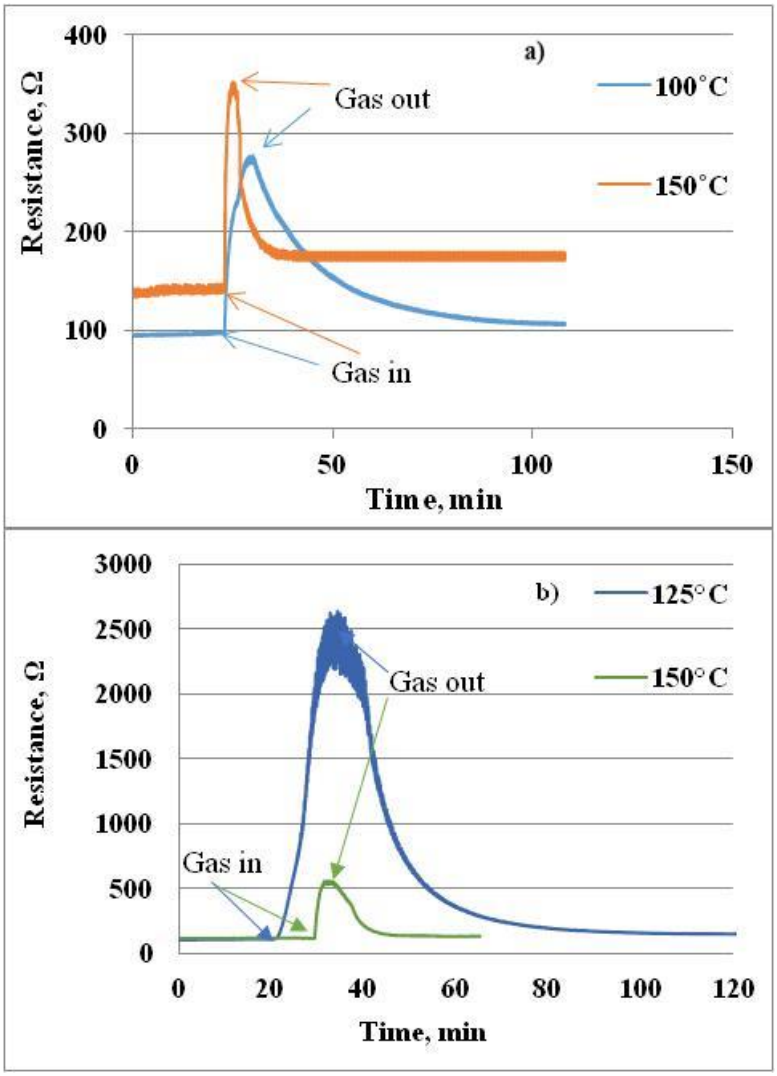

Fig. 7. The response-recovery curves of SnO_2<Co> sensor observed under the influence of 875 ppb (a) and 3.5 ppm (b) of H_2O_2 vapors measured at different operating temperatures.

Despite the fact that the sensor response is higher at 125^0C than that of at 150^0C, the response and the recovery times are almost 6 and 3 times less at 150^0C, respectively. As seen from Fig. 8b, further increase of the gas-sensitive film temperature leads to decrease of response and recovery times.

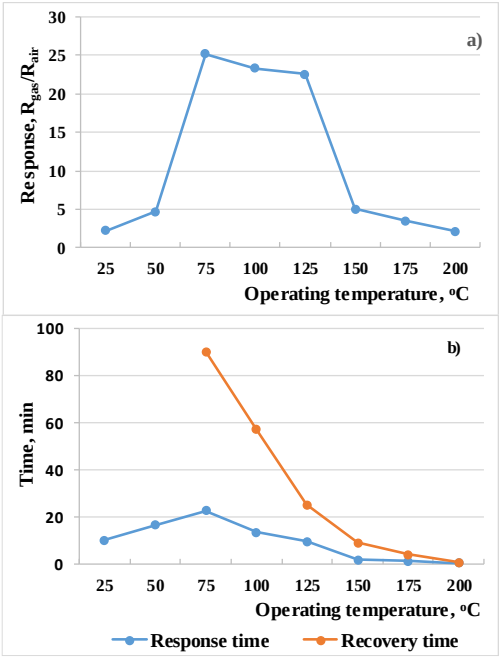

Fig. 8. a) The dependence of the SnO_2<Co> sensor response on the operating temperature at the 3.5 ppm H_2O_2 vapors; b) the dependences of the sensor response and recovery times on the operating temperature.

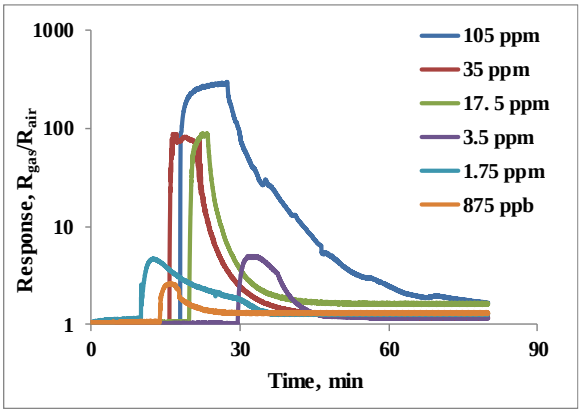

Fig. 9. The sensitivity curves of SnO_2<Co> sensor observed under the influence of different concentrations of H_2O_2 vapors at 150 °C operating temperature.

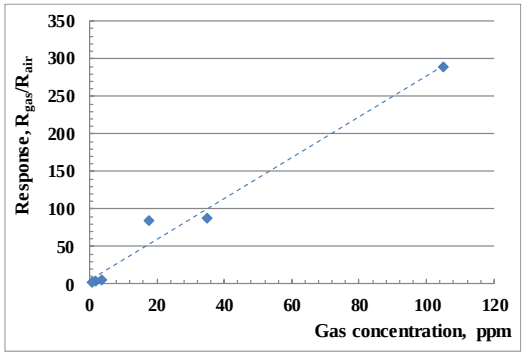

Fig. 10. The dependence of the SnO_2<Co> sensor response on the H_2O_2 vapors concentration.

The sensitivity curves of $SnO_2 < Co >$ sensor observed under the influence of different concentrations of H_2O_2 vapors measured at $150^0 C$ operating temperature are presented in Fig. 9. The sensitivity increases from 2.15 to 290 when the H_2O_2 concentration changes from $875 ppb$ to $105 ppm$.

The dependence of response on the H_2O_2 vapors concentration at $150^0 C$ operating temperature is presented in Fig. 10. The dependence has almost linear characteristics which will allow us not only to detect low concentrations of H_2O_2 vapors but also to accurately measure the concentration.

The dependences of the sensor response and recovery time on the H_2O_2 vapors concentration at $150^0 C$ operating temperature were also extracted (Fig. 11). As seen, with the increasing in H_2O_2 vapors concentration, the response and recovery times do not change significantly, but the response times are relatively smaller compared to the recovery times.

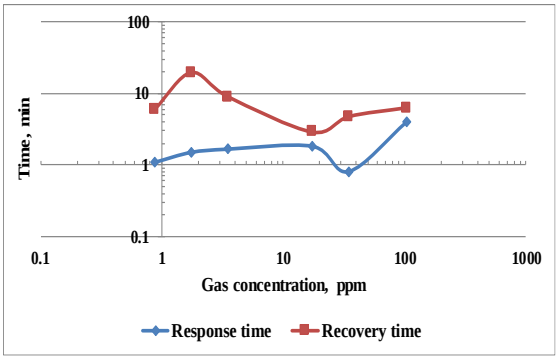

Fig. 11. The dependences of the sensor response and recovery times on the H_2O_2 vapors concentration.

The sensing results at $150^0 C$ operation temperature obtained in this study are presented in Table 2. The sensor made of doped $SnO_2 < Co >$ showed sensitivity to $875 ppb$ H_2O_2 concentration and even in such a low concentration the resistance changed more than twice. The sensitivity of the $SnO_2 < Co >$ sensor varies approximately 300 times in relatively higher

concentrations $(105\,ppm)$ of H_2O_2 vapors, which is also a reliable result. The response times are mainly less than two minutes which is really short for this type of sensor, but the recovery times compared to the response times are longer.

Table 2. The sensing performance of the SnO_2<Co> sensor tested at 150 °C operating temperature.

H_2O_2 vapors concentration, ppm	**Respons, R_{gas}/R_{air}**	**Response time, min**	**Recovery time, min**
105	290	4.1	6.3
35	87.43	0.8	4.75
17.5	84.5	1.83	2.88
3.5	5	1.66	9
1.75	4.22	1.5	19.5
0.875	2.15	1.08	6

4. Conclusions

We have developed and characterized $SnO_2 < Co >$ based thin film sensor using high frequency magnetron sputtering method for H_2O_2 vapors sensing. The chemical analysis showed that the gas sensitive film had $Sn_{0,987}Co_{0,013}O_2$ composition. The $SnO_2 < Co >$ film thickness was equal to 138 nm. The average size of nanoparticles was equal to $18.7\,nm$. The sensitivity of the sensors was improved by sputtering palladium catalytic particles on the surface of the sensing layer. The gas sensing properties of the prepared $SnO_2 < Co >$ sensors were investigated under the influence of the different concentration of H_2O_2 vapors at different operation temperatures. The sensor had sensitivity to $3.5\,ppm$ H_2O_2 vapors even at room temperature. The dependence of response on the H_2O_2 vapors concentration had almost linear characteristic at 150 °C operating temperature. The sensor made of $SnO_2 < Co >$ exhibited high sensitivity, fast response and recovery behavior at the ppb level of H_2O_2 vapors.

References

[1] G. Yu, W. Wu, X. Pan, Q. Zhao, X. Wei, Q. Lu, Sensors 15, (2015) 2709.
[2] J. Agrisuelas, M. González-Sánchez, E. Valero, Sensors and Actuators B 249, (2017) 499.
[3] D. Lee, S. Choi, Y. Byun, Sensors and Actuators B 256, (2018) 744.
[4] B. Patella, R. Inguanta, S. Piazza, C. Sunseri, Sensors and Actuators B 245, (2017) 44.
[5] A.L. Verma, S. Saxena, G.S.S. Saini, V. Gaur, V.K. Jain, Thin Solid Films 519, (2011) 8144.
[6] V.M. Aroutiounian, Sensors and Transducers 223, (2018) 9.
[7] D. O'Sullivana, K.C. Silwal, A.S. McNeill, V. Treadawayc, B.G. Heikes, International Journal of Mass Spectrometry 424, (2018) 16.
[8] B. Puértolas, A.K. Hill, T. Garcíaa, B. Solsonac, L. Torrente-Murciano, Catalysis Today 248, (2015) 115.
[9] P. Kačer, J. Švrček, K. Syslová, J. Václavík, D. Pavlík, J. Červený, M. Kuzma, InTech, Chapter 17, (2012) 399.
[10] S. Corveleyn, G.M.R. Vandenbossche, J.P. Remon, Pharmaceutical Research 14, (1997) 294.
[11] P. Salazara, V. Ricoa, A. R. González-Elipea, Electrochimica Acta 235, (2017) 534.
[12] B.P. Garreffia, M. Guoa, N. Tokranovab, N.C. Cadyb, J. Castracaneb, I.A. Levitskyc, Sensors and Actuators B 276, (2018) 466.
[13] F.I. Bohrer, C.N. Colesniuc, J. Park, I.K. Schuller, A.C. Kummel, W.C. Trogler, Journal of the American Chemical Society 130, (2008) 3712.
[14] J. N'Diaye, S. Poorahong, O. Hmam, R. Izquierdo, M. Siaj, Journal of Electroanalytical Chemistry 789, (2017) 85.
[15] T.A. Miller, S.D. Bakrania, C. Perez, M.S. Wooldridge, Eds. K.E. Geckeler, E. Rosenberg, American Scientific Publishers, Chapter 30, (2006) 1.
[16] A. Klein, C. Korber, A. Wachau, F. Sauberlich, Y. Gassenbauer, S.P. Harvey, D.E. Proffit, T.O. Mason, Materials 3, (2010) 4892.
[17] A. Dey, Materials Science and Engineering B 229, (2018) 206.
[18] V.M. Aroutiounian, V.M. Arakelyan, E.A. Khachaturyan, G.E. Shahnazaryan, M.S. Aleksanyan, L. Forro, A. Margez, K. Hernadi, Z. Nemeth, Sensors and Actuators B 173, (2012) 890.
[19] W. Zhao, J. Jin, H. Wu, S. Wang, C. Fneg, S. Yang, Y. Ding, Materials Science and Engineering C 78, (2017) 185.
[20] G. Korotcenkov, Sensors and Actuators B 244, (2017) 182.
[21] V.M. Aroutiounian, V.M. Arakelyan, M.S. Aleksanyan, G.E. Shahnazaryan, A.G. Sayunts, B. Joost, In the Proceedings of the Conference on '4th International Conference on Sensors Engineering and Electronics Instrumentation Advances (SEIA' 2018)', Amsterdam, The Netherlands, 19-21 September (2018) 49.
[22] A. Rothschild, Y. Komem, Journal of Applied Physics 95, (2004) 6374.
[23] C. Wang, L. Yin, L. Zhang, D. Xiang and R. Gao, Sensors 10, (2010) 2088.
[24] M.S. Aleksanyan, V.M. Arakelyan, V.M. Aroutiounian, G.E. Shahnazaryan, Journal of Contemporary Physics (Armenian Academy of Sciences) 46, (2011) 86.
[25] Sh. Gong, J. Liu, J. Xia, L. Quan, H. Liu, D. Zhou, Materials Science and Engineering B 164, (2009) 85.
[26] Z. Adamyan, A. Sayunts, V. Aroutiounian, E. Khachaturyan, M. Vrnata, P. Fitl, J. Vlček, Journal of Sensors and Sensor Systems 7, (2018) 31.